Production of a Chemically-Bound Dimer of 2,4,6-TNT by Transient High Pressure

Ray Engelke,* Normand C. Blais, Stephen A. Sheffield, and Robert K. Sander

MS P952, Los Alamos National Laboratory, Los Alamos, New Mexico 87544

Received: February 7, 2001; In Final Form: April 16, 2001

We report experimental observations of a chemically bound dimer of 2,4,6-trinitrotoluene (TNT) produced by high-pressure shock waves. The experimental observations were made with a time-of-flight (TOF) mass spectrometer within which it is possible to produce strong shock waves by detonating condensed-phase explosives. The dimer is thought to arise from a Diels−Alder (DA) cross-linking of two TNT molecules. It is noteworthy that DA reactions are strongly pressure enhanced. We found that under some shock conditions a significant fraction of the TNT molecules are dimerized. The dimerization reaction, which is endothermic, may play a role in the shock insensitivity of TNT. Ancillary experiments in which TNT was evaporated and expanded through a nozzle into the mass spectrometer are also reported. It was possible in these experiments to produce a weakly bound TNT dimer in which the binding forces are those characteristic of a crystal. We show that this type of dimer has a different fragmentation pattern caused by electron impact ionization than the one produced by a shock wave. A rough estimate of the binding energy of this type dimer is given. The difference in the fragmentation patterns of the two types of dimer indicates that the dimer produced in the shock wave experiments is a physically different structure than the weakly bound species produced in the evaporation experiments. This supports the view that the shock-produced dimer is chemically bound. Two-dimensional time-dependent reactive hydrodynamic modeling of the shock wave experiments is used to produce estimates of the pressure and temperature fields in the shocked TNT as a function of space and time. The calculations, in conjunction with the experimental data, allow us to estimate the time scale of the shock-wave-produced TNT dimerization reaction as being roughly 10 ns.

I. Introduction

Earlier high-pressure shock wave studies of aromatic structures indicate that they undergo a characteristic chemical cross-linking reaction (a dimerization) that is associated with the pi-bonding structure of the underlying ring structure (see Section II. Background). The earlier studies of this phenomenon were done on molecules that are not capable of decomposing with a large energy release (e.g., anthracene). In the current study, we seek to extend such work into the realm of molecules that are highly energetic; i.e., molecules that can decompose explosively. We chose 2,4,6-trinitrotoluene (TNT) as the subject of such a study. Time-of-flight (TOF) mass spectroscopy was used to obtain the experimental information discussed.

We subjected pellets of solid TNT to high-pressure shock waves. These shock waves were induced into the explosive via electrically driven thin slappers−(see Section III. Experimental Aspects). The impact of the slappers with the explosive samples produced high-pressure (ca. 160 kbar) short-duration (ca. 30 ns) pressure pulses in the struck explosive.

Two different shock wave regimes were examined. First, TNT samples were stimulated by the slapper only. This produced a regime in which the shock wave was supported by the exothermicity it induced, but this exothermicity was not capable of producing a self-sustaining detonation wave. In the second situation, the slapper was used to detonate a more sensitive explosive and the detonation wave thus produced was used to introduce a stronger shock into the TNT than the slapper alone. This arrangement produced a detonation wave in the TNT pellet.

The two methods of introducing shock waves into the TNT pellets produced qualitatively different mass spectra. In the case with weaker shocking, a large amount of dimerization was observed. In contrast to this, when the shock wave introduced produced a propagating detonation, none or only a small amount of dimer was observed in the mass spectra (see Section IV. Results).

We also did experiments in which evaporated TNT was introduced into the mass spectrometer in order to obtain a reference fragmentation pattern for TNT. In these experiments, we were able to produce a weakly bound dimer. An estimate of its binding energy is given in the Appendix.

In Section IV C, the results of two-dimensional reactive compressible-flow calculations of the two types of shock wave experiments are presented. These calculations allow one to estimate the pressure and temperature conditions necessary for producing the chemically bound dimer. An estimate of the time scale of the chemical reaction leading to the shock-wave-produced dimer is given.

Finally, in Section V, we draw conclusions based on the experiments and calculations. The most important inference we make is that TNT's insensitivity to shock wave initiation of detonation may be attributable to its ability to chemically endothermically cross-link. Such a process is an energy sink for shock wave energy and, thus, acts to make the material harder to initiate.

II. Background

There is a significant body of information that indicates that aromatic compounds undergo a characteristic chemical reaction

* Author to whom correspondence should be addressed.

10.1021/jp010492h CCC: $20.00
Published on Web 06/21/2001

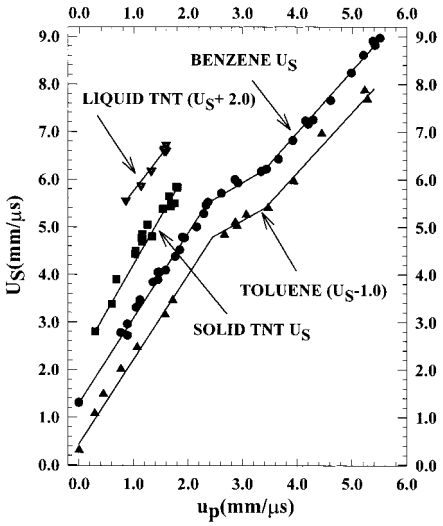

Figure 1. This figure shows the U_S-u_p Hugoniots for benzene and toluene; 1 mm/μs has been subtracted from the U_S values of toluene in order to offset it from the benzene Hugoniot. The graphs show the slope discontinuities characteristic of aromatic structures. The known points for the shock Hugoniots of liquid[8] and solid[9] TNT are also shown; 2 mm/μs has been added to the U_S values of liquid TNT in order to offset it from the other data. The pressures at the 1st and 2nd cusps on the benzene Hugoniot are at ca. 120 and 200 kbar, respectively.

when strongly shocked (i.e., to pressures greater than ca. 120 kbar). The earliest evidence of such a reaction was uncovered when measurements of the shock Hugoniots of some aromatic compounds were made. The principal shock Hugoniot of a material is the locus of all thermodynamic states reachable by a single shock wave from ambient conditions. Dick[1] and Warnes[2] experimentally obtained the principal shock Hugoniots of the ring structures benzene, toluene, anthracene, phenanthrene, pyrene, 1,4-cyclohexadiene, cyclohexene, and cyclohexane up to pressures of ca. 400 kbar. The first five of these structures contain aromatic rings, while the last three do not. These observations are of interest because *all* the molecular species that contain aromatic rings showed slope discontinuities in their principal shock Hugoniots (e.g., see Figure 1), while the three species without aromatic rings present (mentioned above) do not.

When the U_S-u_p data in Figure 1 are replotted in the pressure (P) vs specific volume (v) plane (see ref 1) one sees that the aromatic materials become significantly more compressible at the 1st cusp in the Hugoniot and very incompressible above the 2nd cusp. That is, aromatic materials soften significantly at the 1st cusp—this behavior points to a rate process in which a more compact form of the material is being produced. Dick[1] suggested that a polymerization reaction might be starting at the 1st cusp. Warnes,[2] via chemical analysis of materials recovered from experiments in which anthracene was strongly shocked, found molecules of nearly twice anthracene's molecular weight and suggested that molecular cross-linking could be occurring.

A further point of interest is that Nellis et al.[3] have shocked benzene to over 710 kbar and found no further slope discontinuities on its Hugoniot; i.e., there are no further rapid changes in benzene's compressibility above the 2nd cusp on its Hugoniot (at ca. 200 kbar).

Yakushev et al.[4] did a study of nitrobenzene's (NB) Hugoniot and saw behavior similar to that found with benzene. There is cusp behavior on NB's Hugoniot at ca. 130 kbar that shows a marked increase in the material's compressibility. The volume decrease over the cusp region is -2.6 cm^3/mol. They found optical evidence that this is *not* the result of solidification, since the volume reduction due to solidification is ca. 10 times smaller than the observed effect. Using dielectric measurements on shocked NB, they found indirect evidence that NB molecules are associating; they hypothesized that the associated form was a dipole−dipole dimer.

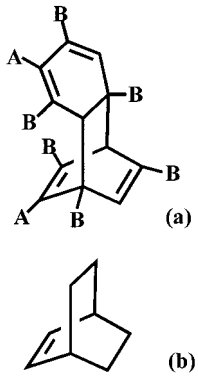

Figure 2. (a) The Diels−Alder cross-linked dimer. In the benzene case, A = B = hydrogen. In the TNT case, the likely dimer, based on electronegativity considerations of the benzene ring side groups, is shown; here A = CH_3 and B = NO_2. CH_3 is electron donating to the ring and NO_2 is electron abstracting, (b) see the text.

Because of the apparent generality of the cusp behavior in shocked aromatics and of the conclusivness of the Hugoniot experiment results, quantum chemical calculations were subsequently done on two benzene molecules to try to determine what cross-linking reactions were consistent with the data. Calculations were done on four structurally distinct chemically cross-linked dimers.[5] One of these structures (*p,p′*-dibenzene) gave a volume decrease (based on a simple model of the shock-compression process) that was consistent with the experimental observations. However, the calculated energy required to surmount the calculated activation barrier leading to this dimer was found to require essentially all of the internal energy change produced by shocking to the 1st cusp on benzene's Hugoniot; this seemed to make the dimerization hypothesis unlikely.

Later, it was noted that all the dimers computed in ref 5 corresponded to symmetry-forbidden reactions and, therefore, have high-energy transition states. It was further noted that there is a symmetry-allowed Diels−Alder (DA) dimerization of benzene that leads to the structure shown in Figure 2a; i.e., *o,p′*-dibenzene-(tricyclo[6.2.2.0^{2,7}]dodeca-3,5,9,11-tetraene). Quantum-chemical calculations on the transition state leading to this structure were consistent with the internal energy changes produced by shocking to the 1st cusp on benzene's Hugoniot.[6] DA reactions have large *negative* volumes of activation and reaction and are strongly pressure enhanced (e.g., by shock pressurization). Furthermore, analogous reactions can occur in *any* aromatic structure.

We note that Dick[1] also determined the principal Hugoniot of 1,3-cyclohexadiene up to 411 kbar and found no evidence of cusps on its Hugoniot. This material can undergo a DA cross-linking. Our hypotheses on why the DA process is not seen in this material is that steric problems due to the nonplanarity of its ring and the reduction in the number of ways the cross-linking can occur so decreases the rate of reaction that it does not occur on the ca. 1 μs time scale of Dick's experiments.

At this point what was needed was experimental evidence at the molecular level that high shock pressure can actually produce dimers. This question was addressed in ref 7 where a mass-spectral study of strongly shocked anthracene crystals was presented. We found that shocking above (below) the 1st cusp

in anthracene's Hugoniot did (did not) produce a chemically bound dimer of anthracene. This is strong experimental evidence in favor of the cross-linking hypothesis. We have also observed a dimer of toluene, produced by shocking liquid toluene, in the same apparatus; this work will be discussed elsewhere.

In this paper, we examine whether an analogous cross-linking occurs in the highly energetic (explosive) material 2,4,6-trinitrotoluene (TNT). The choice of TNT as the candidate energetic material to examine follows from its aromatic structure and its importance as an explosive. The test of the cross-linking reaction using the TNT Hugoniot as a diagnostic is not possible. This is because when one shocks TNT with planewave sustained shocks into the pressure region where cusp behavior is expected (i.e., > ca. 100 kbar), detonation occurs very rapidly relative to the time scale of the mechanical experiments (that have been done to date). Hugoniot data for liquid[8] and solid[9] TNT are shown in Figure 1 to illustrate this point.

In contrast, the hydrodynamic quenching produced in the detonation mass-spectrometer experiments to be described is rapid—see refs 7 and 10. In addition, in our experiments, one obtains information on the mass of the molecular species that are present in the flow produced by the shock wave; such information is absent from mechanical measurements.

III. Experimental Aspects

(A) Shock Experiments. The apparatus and the procedure used to study TNT and its dimers are similar to that used in work we reported previously.[7,10] Briefly we fired small pellets of pressed TNT powder, fastened to a "slapper-barrel" detonator assembly,[7] and mounted inside a high vacuum chamber of the spectrometer. The shock induced into the end of the pellet (fastened to the barrel) by the slapper, is strong enough to either detonate the TNT or to partially exothermically react it into an adiabatically expanding vapor. In either case, the kinetic energy is high enough that the expansion of the gases we sample become highly directed in the shock direction and collisionless. The apparatus is designed so that we can form a sample of these gases into a molecular beam that is directed into a TOF mass spectrometer. A mass spectrum ranging from $m = 0$ to $m =$ 290 amu is taken every 12 μs. This allows us to examine the change in the composition of the products from successive layers of the shocked TNT charge as they arrive at the ionizer of the instrument.

Whether the pellet vaporizes or detonates depends on the shock pressure applied to the end of the pellet. Our pellets contained about 100 mg of material. They were 5-mm diameter and 3-mm long and had a density of 1.55 ± 0.02 gm/cm^3. When fastened to a slapper/barrel assembly alone, the shock strength produced by the slapper and/or its duration was (were) insufficient to bring about detonation of the TNT; however, it did partially react the material. To ensure detonation of the TNT we found it necessary to boost the TNT pellet with a 5-mm diameter $\times$ 0.5- to 1.0-mm thick layer of PETN (pentaerytritol tetranitrate) explosive which was inititiated by the slapper/barrel assembly. This was done by pressing hybrid PETN/TNT pellets. Since PETN is a more sensitive explosive than TNT, it detonates readily and serves as a booster to the shock introduced into the TNT sufficient to produce detonation. In all of the shots we report, the slapper was Kapton plastic 75-μm thick and 3-mm in diameter. The slapper speed upon impact with the pellet surface ranged from 3.75 to 4.25 mm/μs depending on whether the barrel length of the slapper assembly was 1 or 2 mm.

(B) Evaporation Experiments. We also report results obtained by forming a molecular beam by heating (evaporating) the TNT and mixing it with Ar gas. The TNT was heated in a stainless steel cell at 225 °C into Ar carrier gas; the total pressure of the combined gases was ca. 20 KPa. This process results in a mixture of about 20/80% TNT/Ar (by number density). This mixture was expanded through a 0.125-mm diameter nozzle into the vacuum of the TOF spectrometer. By varying the nozzle temperature from 160 to 230 °C, we could change (inversely) the fractional constituency of TNT dimers in the molecular beam entering the detector. We found it necessary to heat the skimmer to ca. 150 °C to prevent condensation of the TNT in the aperture; such condensation cuts off the entry of beam into the detector. Data acquisition for each nozzle temperature was at a slower rate than when taking the shock data. In the evaporation experiments, 16 000 scans were accumulated in memory at the rate of 200 μs per scan and digitized at 4 ns per channel. Since all other parameters of the mass spectrometer are the same as when taking the shock data, about 4800 channels are necessary to observe the TNT evaporation dimer at $m = 454$ amu.

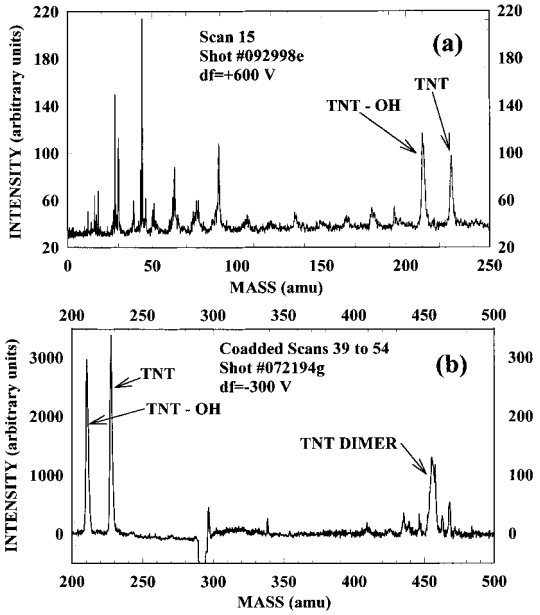

Figure 3. (a) This panel is a scan from a TNT experiment (Shot #092998e) in which no dimers were observed; the TNT parent peak is at $m = 227$ amu. Note the complexity of TNT's cracking pattern; some of the light mass peaks (e.g., at 18, 28, and 44 amu) are from reacted TNT. (b) This panel shows results from an experiment where TNT dimer was observed. The charge in this experiment was initiating *not* detonating. Data from sixteen scans have been co-added in order to make visible some of the small daughter peaks that result from cracking the TNT dimer (e.g., [TNT dimer$-NO_2$] (@ 408 amu), [TNT dimer$-$NO] (@ 424 amu), and [TNT dimer$-H_2O$] (@ 436 amu). Light mass molecules from the scan corresponding to the visible fiducial mark also appear near the dimer peak; the clearest of these correspond to CH_2/N (@ 447 amu), OH (@ 463 amu), and H_2O (@ 468 amu), respectively. Note the large change in the relative areas of the 210 (TNT$-$OH) and 227 (TNT) peaks that occurs when the TNT dimer is present. In the labeling of this figure, df is the deflection voltage applied to the ions.

IV. Results

(A) Shock Wave Experiments. Figure 3a shows a mass spectrum from a *detonating* TNT pellet. Figure 3b shows a mass spectrum that is typical of shots that we characterized as *initiating*, i.e., a spectrum in which the initial shock was sufficient to vaporize the TNT pellet, but which is insufficient to cause detonation. This behavior is considered in detail in the section on the fluid dynamic calculations (see Section IV C).

Above we use the term initiating because it is clear that more than mere vaporization of the material is involved: chemical reactions are occurring in the shocked material that would lead to detonation if the shock were of higher pressure or longer duration. Consequently, the spectra of initiating and detonating TNT have some similarities, consisting of ions of reaction products and of undetonated TNT. However, they can be distinguished from each other because the speeds of the resultant molecular beams are very different. The first molecules to arrive at the detector from a detonating TNT pellet occur at scan 10 after the slapper was energized: these molecules have a speed of about 12 mm/μs. In contrast, the first molecules to arrive from an initiating pellet occur at scan 25 and they have a speed of ca. 4 mm/μs. In addition, the lateral pressures when the pellet detonates are much higher than for initiation and, thus, the lateral expansion of the gas cloud/molecular beam is more rapid. Consequently, we obtain 13 or 14 useful spectral scans if the pellet detonates, but 30 or more useful scans if the pellet initiates. The spectrum shown in Figure 3a is rich because the TNT molecule fragments extensively upon electron-impact ionization. Note that many of the ions with masses 46 amu or less in this spectrum are reaction products from the shock-induced chemistry. However, some of the observed ions are fragmentation products of undetonated TNT molecules. Ions with masses in the range $m = 50$ to $m < 227$ are such electron impact fragments; $m = 227$ mass is the parent TNT ion. Each TNT molecule that ionizes can appear as an ion at any of the masses in TNT's fragmentation pattern; this dilutes the apparent TNT constituency in the product beam. There were no detectable TNT dimers in the mass spectrum of the experiment shown in Figure 3a.

Important changes in the TNT spectrum occur when dimers are present. This is illustrated in the four panels of Figure 4. These panels show the spectra observed in four successive scans of one shot in which the TNT pellet was initiating (i.e., *not* detonating). Note the change in the relative proportions of masses 210 and 227 as the intensity of the dimer peak (at $m =$ 454) increases in successive scans. When several shots of this kind are averaged, we find that the 227 ion signal becomes as large or exceeds that of 210 signal—as the dimer intensity becomes as large as the 210 ion signal. Panel b of Figure 3 illustrates this point. It is the averaged spectra of 16 scans starting at scan 39 of a shot similar to that shown in Figure 4. Two shots in particular were fired under instrument conditions that were suitable for quantitative measurements in the high mass range. The one used in Figure 4 was one of them. When we average over a total of 24 scans, the ion signals at 210, 227, and 454 amu are in the ratio 1.00:1.08:0.81. No other relative intensities between other ion signals appear to change this dramatically when dimer is present. The simplicity of the spectra (see Figures 3b and 4) in the mass region between the dimer and the parent peak of TNT is striking. When the dimer fragments upon ionization, it appears to produce preponderantly ions of the parent TNT molecule.

The negative signal at $m = 290$ in Figure 4 is a fiducial mark; such marks appear at the start of each scan of the mass spectrum. It appears in this plot because the time-of-flight of the TNT dimer places it in the early portion of the scan following the scan in which the ion is formed. This is due to its high mass and consequent low speed toward the detectors. Some of the narrow peaks near the dimer parent seen in Figure 3b are from light mass ions formed at the start of the scan whose fiducial mark is shown on the figure. The apparent masses of some of these low mass ion peaks are given in the figure caption of Figure 3b. Some of the TNT dimer daughter peaks are also identified on this figure. We note that the neutral dimers of TNT in this shot have acquired a kinetic energy of as much as 18 eV, when the molecular beam became collisionless.

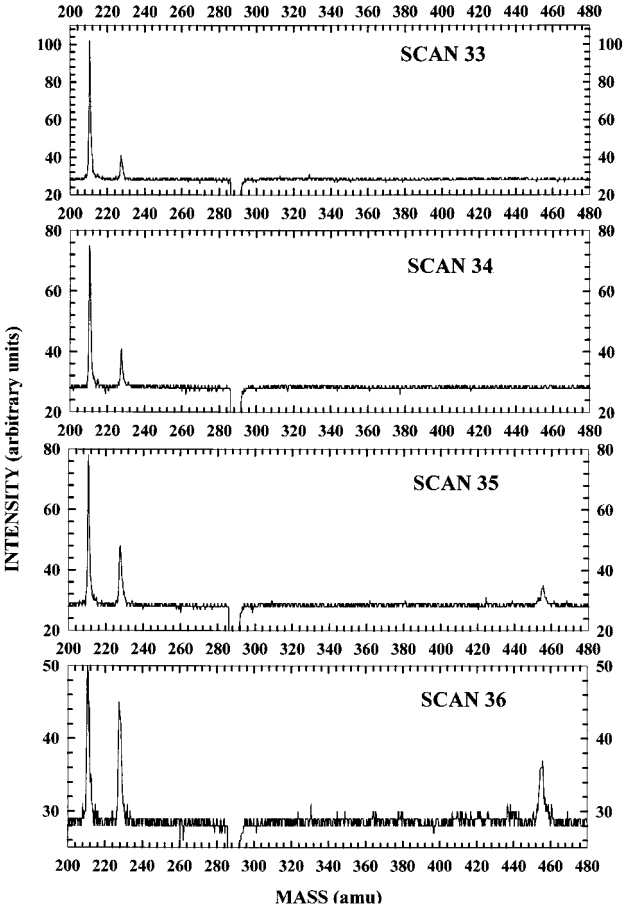

Figure 4. Plots from four successive scans of Shot #071698b. The change in the areas of the 210 and 227 peak areas in going from scan 33 to scan 34 suggests that some dimer is present at scan 34—but the amount remaining unfragmented is too small for us to detect. Scans 35 and 36 show the growing-in of substantial amounts of TNT dimer as time progresses. Given the strong evidence of substantial fragmenting of the TNT dimer into $m = 210$ and 227 amu species, scan 36 is evidence of a *substantial* amount of TNT monomer being converted into TNT dimer in *initiating* TNT.

We confirmed the identity of the TNT dimer signal and that of its daughters shown in Figure 3b by eliminating any light masses that overlap the late-arriving dimer ions and their fragments. We accomplished this by repeating the initiation shots with a suitable setting of the ion deflection voltages at the ionizer section of the mass spectrometer.[10] We show the values of the deflection voltage used to obtain the mass spectrum on each panel of the Figure 3.

Given the above observations, it is of interest to examine the electron-beam fragmentation patterns of other parent molecules that are produced by DA reactions to see whether they exhibit parallel fragmentation behavior. That is, do molecules produced by DA reacting a diene and a dienophile tend to produce ions of the diene moiety preferentially when struck by an electron beam? The molecule closest in structure to the hypothetical TNT dimer parent (see Figure 2a) that we could find in the NIST Chemistry WebBook[11] collection of fragmentation patterns is shown in Figure 2b. This molecule (bicyclo[2.2.2]oct-2-ene) can be formed by the DA reaction of 1,3-cyclohexadiene (the diene) with ethylene (the dienophile). The predominant ion produced when a 70-ev electron beam strikes the bicyclo compound is

1,3-cyclohexadiene; ca. 7.7 times more 1,3-cyclohexadiene than the parent bicyclo compound is found in the fragmentation pattern of the bicyclo parent.

Similar strong production of the diene moiety is observed when such an electron beam strikes cyclohexene and 4-ethenyl-cyclohexene; i.e., strong signals of the butadiene ion are observed. Cyclohexene and 4-ethenyl-cyclohexene are obtained by the DA reactions of butadiene and ethylene and of butadiene and butadiene, respectively; the diene being butadiene in both cases.

These observations support the evidence presented above that a significant portion of the shock-produced TNT dimer fragments to produce some of the ion peak intensity we observe at 227 amu. Therefore, if one wishes to obtain a quantitative estimate of the amount of TNT dimer produced by a shock wave, one needs to correct for the loss of TNT dimer signal due to this fragmentation process.

(B) The Evaporation Experiments. Because the mass spectrum of the fragmentation pattern of TNT is complex, it is advisable to have a reference spectrum that is obtained under the same mass spectrometer operating conditions as those of the shock studies. We obtained such a spectrum by evaporating TNT into the mass spectrometer. With this spectrum, we can separate the ion signals that arise from unreacted TNT from those that arise from chemical reactions caused by the shock. Our evaporation experiment results are qualitatively similar to those of earlier workers,[12−14] except for a noteworthy difference in the reported ratio of the 227/210 ion mass intensities. The spectra of refs 12, 13, and 14 are in substantial agreement with each other on this point, each giving the ratio of 227/210 as about 4%; i.e., they report essentially no parent ion peak (i.e., at 227 amu) in their TNT spectra. All of our spectra give this ratio as much larger. The averaged of this ratio from our shock data is about 39%, while that of our nozzle work is ca. 48%—i.e., much larger than the ratio found by earlier workers. We attribute this to our use of nonstandard ionizer operating parameters (e.g., 90 eV ionization electrons, rather than the more usual 70 eV) and, additionally, in the case of the evaporation dimer, to the weakness of its binding (see the Appendix).

The value of the ratio of the 227/210 ion intensities is an important quantity for our work, because the presence of dimers in the molecular beam has a large effect on this ratio. In fact, the gas-phase dimers affect the ratio more strongly than those formed in the shock experiments. Evidently in the gas-phase experiments, as for the shock studies, the fragmentation of the evaporation dimer predominantly populates the TNT parent ion peak.

A plot of the 227/210 peak−area ratio as a function of the 454/210 peak−area, as obtained from the evaporation experiments, is shown in Figure 5. An extrapolation of the linear fit to the data, shown in the figure, indicates that the 227/210 ratio would become unity when the 454/210 ratio is 7%. This is about 10 times less than the amount of shocked dimer needed to change the 227/210 data to the same ratio. We use these changes in the 227/210 ratio as a function of the 454/210 ratio to estimate the amount of fragmentation occurring in the ionization of the dimers found in each of the experiments, shocked or evaporated. If we assume that the ions at masses 210, 227, and 454 are detected with the same efficiency, and that both dimers fragment mostly to mass 227, we find that the shocked dimers fragment less than $^1/_2$ as much as the evaporation dimers: i.e., 45% as compared to 90%. This is good evidence that the dimers produced in the two different experiments are physically different structures. If we further neglect any differences in the ionization efficiencies between each kind of dimer ion and the monomer ion, we find that the highest ratios of dimer to monomer produced in our shock and evaporation experiments were 24% and 9%, respectively.

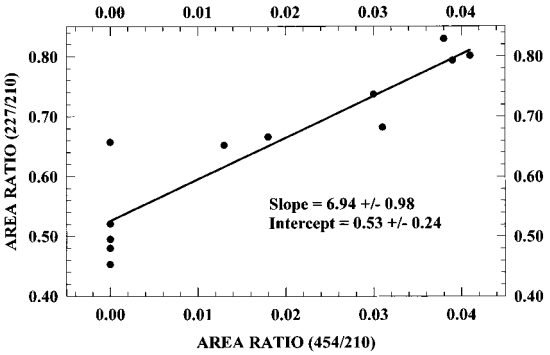

Figure 5. Plot of the trend in the 227/210 peak area ratio as a function of the 454/210 peak area ratio obtained in the evaporation experiments. Both the slope and intercept parameters of the regression line are statistically significant; error estimates are 1σ.

We make a rough estimate of the binding energy of the evaporation dimer in the Appendix.

(C) Computed Fluid-Mechanical Results. The CTH wave propagation code[15] was chosen to do the fluid-dynamical modeling of the experiments. CTH is a mixed Eulerian/Lagrangian code; i.e., the problem is set up in the Eulerian frame and then mapped to the Lagrangian frame, where the fluid motion is calculated for one time step. The results are then mapped back into the Eulerian frame. This process is repeated for each time step. This methodology eliminates some of the problems associated with cell distortion experienced with pure Eulerian codes.

All the calculations were done in two-dimensional cylindrical geometry with the problem setup as close as possible to the experimental arrangements. In the initiation experiments, the shock input to the TNT was ca. 165 kbar; in the detonation experiments, the shock input to the PETN was ca. 250 kbar. To simulate the reaction process in the TNT and PETN, a global (single reaction) rate form was used. This form determines the way chemical energy is released into the flow. The History-Variable-Reactive-Burn (HVRB) model,[16] which is purely empirical, was chosen. This model employs a pressure-dependent rate with a time delay before reaction starts. Pressure is used as the state variable since it is a measurable mechanical quantity whereas the temperature is not. The extent of reaction progress (λ) is given by

$$\lambda = \min(1,\varphi^M),\ \phi = \frac{1}{\tau_0}\int_0^t \left(\frac{P - P_i}{P_r}\right)^z \mathrm{d}\tau$$

where M, P_r, P_i, and z are adjustable parameters calibrated for a particular explosive and τ_0 is chosen to be 1 μs to make λ dimensionless. λ varies from 0 for no reaction to 1 for complete reaction and P is the local pressure.

The initial computations were done with TNT parameters developed previously[17] and they indicated that the TNT would not detonate under any of the conditions used in the experiments (even with the PETN boosting). We adjusted two parameters (P_r and z) in the simulation of the initiation experiments such that the TNT reacted, but did not detonate when the shock wave had reached the free surface of the charge (see the right panels of Figure 6). Simulations, using the revised parameters, of the experiments in which the PETN was added between the slapper

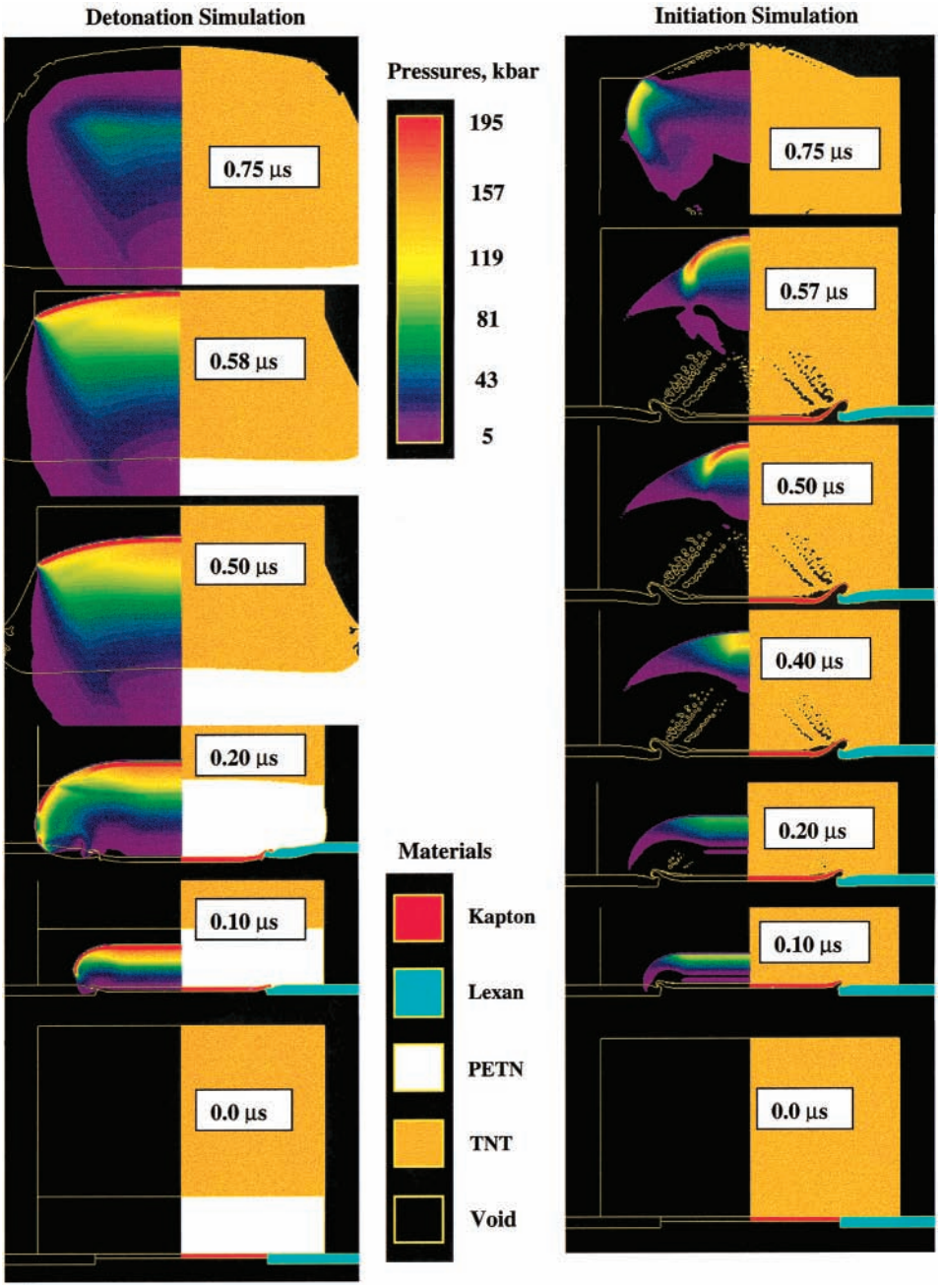

Figure 6. On the left side are several snapshots of the simulation of the detonation experiment at times of 0.0, 0.1, 0.2, 0.5, 0.58, and 0.75 μs. On the right side are snapshots of the simulation of the initiation experiment at times of 0.0, 0.1, 0.2, 0.4, 0.5, 0.57, and 0.75 μs. On the right side of each snapshot the materials are shown (with boundaries) according to the legend in the middle bottom. On the left side of the snapshots are pressures depicted by colors according to the legend in the middle top (from 5 to 200 kbar). Note that the presence of the PETN in the detonation experiment introduces a time offset for the wave motion in the TNT.

and the TNT shows that a detonation wave develops in the TNT (see the left panels of Figure 6).

The unreacted TNT and PETN equation of state (EOS) forms used in all the simulations were a Mie−Gruneisen form with a constant specific heat and density/Gruneisen parameter product. The EOS parameters were adjusted to account for the pressed pellets being less than full density. The TNT and PETN reaction product EOSs were tabular forms based on a mixture−chemical equilibrium model that simulates detonation cylinder expansion experiments.[17] The Kapton EOS was also a Mie−Gruneisen form. Cell dimensions were 20 μm in both the radial and axial directions; this led to calculations with 160 000 cells. Many simulations were done to determine the appropriate HVRB parameters.

A simulation was also done of the initiation experiment in which the TNT was treated as inert. In this simulation, the short-duration shock pulse generated by the Kapton slapper attenuated rapidly from both the back and the sides to the point that there was essentially no shock present when the wave reached the front surface of the charge. This demonstrates that considerable chemical-heat release was present in the experiments where the TNT was "initiating".

Simulations of the initiation experiments in which the TNT was allowed to react show an interesting reaction pattern (see the right panels of Figure 6). The input wave, with a pressure of 165 kbar attenuates from the back as well as the sides in the early stages. As the wave moves through the charge, TNT reaction occurs behind the front and this mitigates the effects

TABLE 1: Details from the Computer Simulations

experiment type	explosive setup/ thick (mm)	Kapton slapper speed (mm/μs)	pressure input to HE (kbar)	pressure 60 μm from free surface (kbar)	free surface speed (mm/μs)[a]	temperature 60 μm from free surface (K)[a]
initiation	TNT/3	3.75	165	170	4.0	2100
detonation	PETN/1 TNT/3	4.25	PETN 285 TNT 325	260	5.1	3600

[a] Value at the time when the shock wave reaches the free surface of the charge.

of attenuation, causing the wave to build in pressure. This begins to occur when the wave had traveled ca. 1 mm into the TNT (between the snapshots at 0.2 and 0.4 μs of Figure 6). The wave continues to build to the point that a localized detonation appears near the centerline of the charge; this occurs when the wave has traveled about 2 mm into the TNT (shortly after the 0.4 μs snapshot in Figure 6). This localized detonation grows radially for a period of time, but then dies out prior to interacting with the free surface (see the snapshot at 0.57 μs of Figure 6). In this simulation, a free surface speed of ca. 4 mm/μs was computed. This is in good agreement with the value of 4.1 mm/μs value that was measured in the experiments. The pressure generated by the wave at a position 60 μm from the charge-free surface is about 180 kbar. This pressure is significantly higher than that at the 1st cusp in the benzene and toluene Hugoniots (see Figure 1) and, thus, by analogy should cause the cusp-related phenomena in TNT. Summary numerical values of this simulation are given in Table 1.

Simulations (using the "initiating" case HVRB parameters) of the experiments with PETN boosting produces a detonation in the TNT (see the panels on the left side of Figure 6). In this case, the Kapton slapper imparts a shock into the PETN that rapidly turns into a detonation (see the snapshot at 0.1 μs). This detonation wave, which is only slightly attenuated from the sides, strongly shocks the TNT and rapidly produces a detonation wave in it. The detonation in the TNT, which is slightly curved, travels through the TNT with only minor changes in shape (see the snapshot at 0.58 μs). The detonation wave interacts with the free surface and produces a free surface speed of 5.1 mm/μs. Summary numerical values of the detonation simulation are given in Table 1.

Based on the results shown in Figure 6, it is clear that the initiating and detonating flows are profoundly different. The free surface speed/time profiles are shown in Figure 7 for both cases. Based on when TNT molecules reached the detectors in the mass spectrometer, the mass speeds in the initiating and detonating cases were 4.1 and 9.8 mm/μs, respectively. The speeds for the initiation experiment and the simulation are nearly the same. The HVRB parameters were adjusted to make this the case. The particle speeds reached in the detonation case simulation were significantly lower than those observed in the experiments. Apparently, this results from deficiencies in the JWL EOS at the lower pressure portions of the expansion. This is not significant for our work since we are interested in the physical states experienced in the high pressure (i.e., >100 kbar) regime. A theoretical discussion of the final state speeds achievable for a detonating material can be found in ref 18. The final speed values of ca. 10 mm/μs derived there are in good agreement with our observations.

The temperatures calculated in the simulations (see Figure 8) can only be considered to be rough estimates because of the assumptions made with respect to specific heat and Gruneisen's parameters characteristics. However, the relative difference in

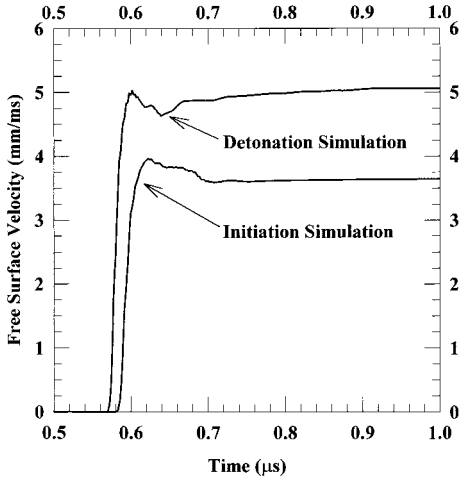

Figure 7. Plot of the free surface speeds as a function of time from both the initiation and detonation simulations.

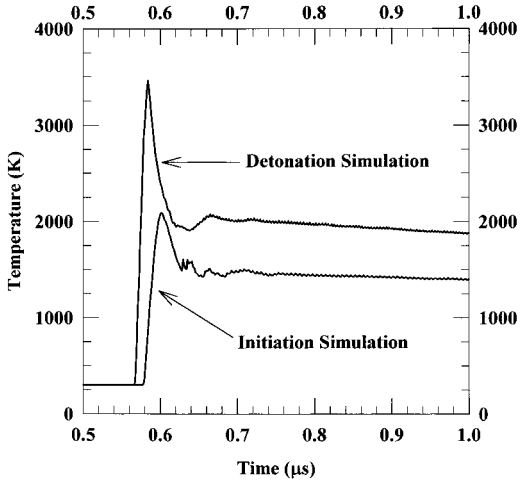

Figure 8. Plot of calculated temperatures as a function of time for Lagrangian points 60 μm from the free surface from both the initiation and detonation simulations. Note that the temperature difference between the two cases is probably a more valid estimate than the temperatures themselves.

temperatures are probably more realistic. The calculations indicate large temperature differences are experienced by the materials in the two types of experiments.

We can make a rough estimate of the reaction time characteristic of the shock produced dimerization as follows. For the shot shown in Figure 3b we found: (1) TNT molecules were first observed at Scan 30, (2) TNT dimers were first observed at Scan 38, and (3) the amount of TNT dimer became constant after Scan 42. In other work we have found that one scan of the spectrometer corresponds to approximately 10 μm in the explosive charge. Therefore, the first observation of TNT dimer and the completed reaction are observed at "particles" that are 80 and 120 μm from the front surface of the charge, respectively. Calculations were done in which the pressure and temperature histories of these particles were followed. We found that the particle initially at 120 μm from the front surface of the charge had its pressure held above 120 kbar about 8 ns longer than the particle at 80 μm from the front surface. The time these two cells are held above any "threshold" pressure is not sensitive to the pressure value assumed; therefore, the value of 8 ns noted above is not sensitive to the assumed pressure value of 120 kbar. In this argument we have ignored the fact that the 120 μm particle is at any time about 500 K hotter than the 80 μm particle; this implies that our reaction time estimate is probably

an under-estimate. It is probably safe to say that the reaction time for producing the dimer in our initiation experiments is ca. 10 ns.

V. Conclusions

We have observed a shock-wave-produced chemically bound dimer of 2,4,6-TNT.

In the TOF mass spectra in which the shock-wave-produced dimer is observed, only very small quantities of other molecular species in the mass region between the TNT monomer parent (at 227 amu) and the TNT dimer parent (at 454 amu) are observed (see Figure 3b). That is, the experimental evidence supports the view that the shock wave produces essentially one species with mass greater than TNT itself. Since the cross-linked dimer is substantially more compact than two TNT molecules, dimer production leads to an increase compressibility of the shocked material. This observation correlates with the 1st cusp behavior in aromatic materials whose principal shock Hugoniots have been measured at pressure in the region of 100 kbar and higher (see Figure 1).

From the proportion of dimer to monomer we estimate to be in the shocked molecular beam material, we compute that ca. 24% of the TNT monomers are converted to TNT dimer when the TNT is initiating. This degree of conversion for the strongly endothermic process which produces the energetically metastable TNT dimer is a substantial energy sink for withdrawing energy from the shock wave, and, thus, for decreasing the shock's strength. A rough estimate of the degree of this endothermicity can be obtained from quantum-chemical calculational results for the formation of the analogous benzene dimer.[6] These calculations predict that the endothermicity of the reaction of two benzenes to the structure shown in Figure 2a (with A = B = hydrogen) is ca. 27 kcal/mol.

Based on earlier experimental and theoretical work on shocked nonenergetic aromatic materials (e.g., benzene, toluene, anthracene, etc.) and on the present work, we think that the best working hypothesis concerning the molecular structure of shock-produced TNT dimer is that shown in Figure 2a. This dimer is the result of a Diels−Alder (DA) cross-linking of two TNT molecules. The position of the NO_2 and CH_3 groups on the hypothesized structure are inferred from the effect on DA reactions of the electron donating and withdrawing character of the side groups. That is, electron-attracting groups (here NO_2) on the dienophile facilitate the reaction, as do electron-donating groups (here CH_3) on the diene.[19] Clearly, there are many stereoisomers possible in the reaction. Therefore, it is possible that the observed dimer spectra are actually due to a combination of the basic dimer structure with the side groups at various other positions; the present experiments do not cast light on this question.

In contrast to the case in which the shock is "initiating", when the TNT detonated (by addition of a PETN booster), only a very small amount (or no) TNT dimer is observed. In this situation, the molecules that are prominent in the observed spectra are lower mass species that mostly correspond to low-energy detonation products (e.g., CO, N_2, H_2O, CO_2, etc.). This suggests that when a shock wave of sufficient strength (and duration) is introduced into TNT, exothermic chemical kinetic processes faster than that which produces the endothermic dimer reaction come into play. If this is correct, it has implications for TNT's shock insensitivity as a solid explosive; this will be discussed further at the end of this section.

To obtain a reference fragmentation pattern for TNT, we also did experiments in which TNT was evaporated into the mass spectrometer. By controlling the temperature of the exit nozzle of the evaporated material, we succeeded in producing a weakly bound dimer of TNT. We think this dimer is the result of dipole−dipole and dispersion forces characteristic of those that bind a TNT crystal. Note that production of this type of dimer is weakly exothermic, while production of the DA dimer is strongly endothermic. We do not believe the weakly bound dimer can survive the rigorous temperature conditions present in the shocked material. The fluid dynamic calculations indicate that even in the "initiating" case, the temperature present in the shocked TNT is greater than ca. 1700 K near the front of the charge. Our calculation of the binding energy of the dimer produced in the evaporation experiments is -1290 ± 162 K (see the Appendix). In the evaporation experiments, an increase of the measured nozzle temperature of less than 50 K eliminated the evaporation dimer—within our ability to detect it. Another factor pointing to the weakness of the binding of the evaporation dimer is the effect its presence has on the relative areas of the spectral peaks at 227 and 210 amu. We compute that ca. 7 times more shock dimer than evaporation dimer is needed to have the same effect on the 227/210 area ratio. This is further evidence that the evaporation dimer is very weakly bound.

2,4,6-TNT is a quite insensitive solid explosive under the conditions described here (e.g., the initial mass density of the pellets fired). We suggest that, at least, some of this insensitivity is attributable to the formation of the strongly endothermic DA dimer we observe when TNT is subjected to an "initiating" shock. This is due to the transformation of shock wave energy into internal chemical energy caused by dimer production with a consequent degradation of the shock strength.

Clearly, if this idea is correct, it has implications for other aromatic-ring-based explosives. For example, the explosive 1,3,5-triamino-2,4,6-trinitrobenzene (TATB) is an even more insensitive explosive than is TNT, even though it can produce higher detonation speeds and pressures. A possible explanation of TATB's shock insensitivity is that it also undergoes the DA dimerization when shocked. In addition, crystals of TATB contain an extensive network of hydrogen bonds (due to the presence of NO_2 and NH_2 groups). It takes shock wave energy to disrupt this hydrogen bond network and also to produce the DA dimer. Consequently, this may be the origin of TATB's greater insensitivity to shock than TNT's. We note that dimers of TATB have also been observed with our apparatus when TATB is strongly shocked.[20]

We suggest that such insights are potentially valuable in the design of new insensitive, but highly energetic, explosive materials.

Appendix

The Binding Energy of the Evaporation Dimer. One can make an estimate of the binding energy of the dimer produced in the evaporation experiments. For a reaction of the type

$$A_2 \rightleftarrows A + A \tag{1}$$

Moore[21] obtains the relationship between the number densities of the dimer (N_{A2}) and the monomer (N_A) based on the equilibrium constant at constant pressure and temperature. We modified his form to

$$\ln\left[\left\{\frac{N_A(T_1)}{N_A(T_2)}\right\}^2\left\{\frac{N_{A2}(T_2)}{N_{A2}(T_1)}\right\}\left\{\frac{T_2}{T_1}\right\}^{1/2}\right] = T^*\left[\frac{1}{T_2} - \frac{1}{T_1}\right] \tag{2}$$

where A_2 and A represent the TNT dimer and monomer,

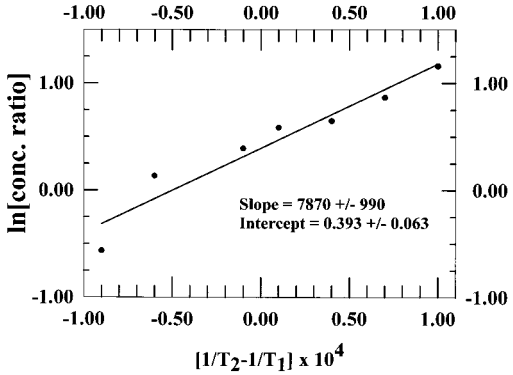

Figure 9. Equilibrium constant data from the evaporation experiments. This predicts a binding energy of the evaporation dimer of ca. 0.11 eV/molecule. The error estimates on the parameters are 1σ.

respectively. Equation 2 uses the ratio of Moore's expression at two different temperatures. By using this modified form, we eliminate the need to rescale our data because of changes in signal intensity with changes in the nozzle temperature and the differences in the ionization cross-sections of the monomer and dimer species. In eq 2, T^* is the "binding temperature" of the dimer, so that its binding energy is $\Delta E = kT^*$, where k is Boltzmann's constant. The 89 amu peak was used as an estimator of the TNT monomer number density because it is a strong peak and its intensity was not observed to be strongly influenced by dimer presence (i.e., by fragmentation of the dimer). The points in Figure 9 are the results of the data reduction on the evaporation experiments in which significant dimer signal was observed. The slope of the semilogarithmic line fit to these data gives a value of $T^* = 7870 \pm 990$ K. The temperatures used in plotting the data in Figure 9 were those measured at the nozzle exit. However, this is not the temperature of the material in the center of the gas flow where condensation of TNT to dimers occurs. We did not have the apparatus available with which to measure that temperature, so the following procedure was used to obtain a reasonable estimate of its value.

Hoffbauer[22] did velocity measurements of Ar gas exiting a nozzle under conditions similar to the ones we used to form our TNT molecular beams (i.e., nozzle orifice diameter and gas pressure). From the distribution of Ar speeds, he found the kinetic temperature to be 8.6 K. When corrected for the higher temperatures used in our nozzles, the Ar temperature for the same Mach number of the expansion is $T_{Ar} = 13$ K. The speed distributions obtained from nozzle expansions of the kind we are describing have the form $P(v) = v^3 \exp((v - v_0)/\alpha)^2$, where $\alpha = (2kT/m)^{1/2}$.[23] By seeding TNT molecules into the Ar flow such that the mole fraction of TNT to Ar is sufficiently small, i.e., ca. 10% or less, the speed distribution of the heavier TNT molecules will have nearly the same distribution as the Ar. In this case, the kinetic temperature of the TNT is given by $T_{TNT} = T_{Ar} m_{TNT}/m_{Ar}$, which when evaluated with our parameters gives $T_{TNT} = 74$ K. This is the kinetic temperature which determines the probability of TNT dimer formation upon a three-body collision of two TNT molecules and an Ar atom in the higher number density region of the nozzle expansion. That is, the kinetic distribution of the TNT molecules is a measure of the amount of energy that must be removed from the TNT−TNT collision coordinate (the incipient TNT dimer bond) by the Ar atom to form a dimer. The intramolecular vibrations of the TNT are generally not relaxed as rapidly as the kinetic modes and play only a minor role in dimer formation. Therefore, the measured nozzle temperature from which we obtained the value of T^* quoted above was reduced by a factor of 6.1 to give a scaled value of 1290 ± 162 K. We consider this to be a lower limit to the dimer binding energy because the amount of seeding of TNT into the Ar carrier gas was probably large enough to alter slightly the TNT speed distribution from that of the Ar by slippage.

Equation 2 is derived with the assumption of equilibrium conditions, i.e., that all the molecular and atomic motions are described by canonical distributions. This can be only approximately true since the system variables of the nozzle expansion, local temperature, number density, etc., are time-dependent in the flow direction. However, our data is satisfactorily represented by a straight line (see Figure 9). Moreover, note that all of the molecular motions important in the dimerization of TNT are low-energy motions that will relax about as rapidly as the translational degrees of freedom. For example, even though the intramolecular vibrations of TNT may not be equilibrated they may not be a serious perturbation to the quantities that we are examining.

Our calculated value of the binding energy of the evaporation dimer is ca. 0.11 eV/molecule (2.6 kcal/mol) and, therefore, it is not a chemically bound species. Our computed value is consistent with the binding energies of other ring structures as determined by other workers. For example, experimentally calibrated theoretical models of the binding energy of weakly bound benzene dimers give values in the range 1160 to 1260 K for some geometrical conformers.[24]

References and Notes

(1) Dick, R. *J. Chem. Phys.* **1970**, *52*, 6021; **1979**, *71*, 3203.
(2) Warnes, R. H. *J. Chem. Phys.* **1970**, *53*, 1088.
(3) Nellis, W. J.; Ree, F. H.; Trainor, R. J.; Mitchell, A. C.; Boslough, M. B. *J. Chem. Phys.* **1984**, *80*, 2789.
(4) Yakushev, V. V.; Dremin, A. N.; Nabatov, S. S.; Shunin, V. M. *Fiz. Goreniya Vzryva* **1979**, *15*, 132.
(5) (a) Engelke, R.; Hay, P. J.; Kleier, D. A.; Wadt, W. R. *J. Chem. Phys.* **1983**, *79*, 4367. (b) Engelke, R.; Hay, P. J.; Kleier, D. A.; Wadt, W. R. *J. Am. Chem. Soc.* **1984**, *106*, 5439.
(6) Engelke, R. *J. Am. Chem. Soc.* **1986**, *108*, 5799.
(7) Engelke, R.; Blais, N. C. *J. Chem. Phys.* **1994**, *101*, 10,961.
(8) Garn, W. B. *J. Chem. Phys.* **1959**, *30*, 819.
(9) *LASL Explosive Property Data*; Gibbs, T. R., Popolato, A., Eds.; University of California Press: Berkeley, 1980; pp 339−343.
(10) Blais, N. C.; Fry, H. A.; Greiner, N. R. *Rev. Sci. Instrum.* **1993**, *64*, 174.
(11) NIST Chemistry WebBook (http:/webbook.nist.gov/chemistry).
(12) Boettger, H. C., http://webbook.nist.gov.
(13) Volk, F. *Explosivstoffe* **1968**, NR 1, 8.
(14) Bulusu, S.; Axenrod, T. *Org. Mass Spectrom.* **1979**, *14*, 585.
(15) McGlaun, M. C.; Thompson, S. L.; Kmetyk, L. N.; Elrich, M. G. *A Brief Description of the Three-Dimensional Shock Wave Physics Code CTH*; Sandia National Laboratories, SAND89-0607, 1989.
(16) Kerley, G. I. *CTH Equation of State Package: Porosity and Reactive Burn Models*; Sandia National Laboratories, SAND92-0553, 1992.
(17) (a) Kerley, G. I. Theoretical Equations of State for the Detonation Properties of Explosives. In *Proceedings of the Eighth Symposium (International) on Detonation*; Short, J. M., Ed.; NSWL MP 86-194 (Naval Surface Weapons Center, White Oak, MD, 1986); pp 540−547. (b) Kerley, G. I., Theoretical Model of Explosive Detonation Products: Tests and Sensitivity Studies. In *Proceedings of the Ninth Symposium (International) on Detonation*;Morat, W. J., Ed.; OCNR 113291-7 (Office of the Chief of Naval Research, 1990), pp 442−451. (c) Kerley, G. I.; Christian-Frear, T. L. *Prediction of Explosive Cylinder Tests Using Equations of State from the PANDA Code*; Sandia National Laboratories, SAND93-2131, 1993.
(18) Ahrens, T. J.; Allen, C. F.; Kovach, R. L. *J. Appl. Phys.* **1971**, *42*, 815.
(19) (a) Streitwieser, A., Jr.; Heathcock, C. H. *Introduction To Organic Chemistry*; Macmillan: New York, 1976; p 624. (b) March, J. *Advanced Organic Chemistry*, 3rd ed.; Wiley: New York, 1985; p 746.
(20) Greiner, N. R.; Fry, H. A.; Blais, N. C.; Engelke, R. *Proceedings of the Tenth Detonation Symposium*; Office of Naval Research Report ONR 33395-12; ONR: Washington, DC, 1995; p 563.

(21) Moore, W. J. *Physical Chemistry*, 4th ed.; Prentice Hall: Englewood Cliffs, NJ, 1972; p 299.
(22) Hoffbauer, M. A. Los Alamos National Laboratory, private communication, Sept. 2000.
(23) Anderson, J. B. *Molecular Beams and Low-Density Gas Dynamics*; Wegener, P. P., Ed.; Dekker: New York, 1974; p 1.
(24) (a) Evans, D. J.; Watts, R. O. *Mol. Phys.* **1976**, *31*, 83. (b) MacRury, T. B.; Steele, W. A.; Berne, B. J. *J. Chem. Phys.* **1976**, *64*, 1288.